Improved Plasma Performance in Tokamaks with Negative Magnetic Shear

C. Kessel, J. Manickam, G. Rewoldt, and W. M. Tang

Plasma Physics Laboratory, Princeton University, Princeton, New Jersey 08543-0451

A tokamak plasma configuration is reported that simultaneously improves on the maximum stable plasma pressure, the bootstrap current contribution, and kinetic stability to temperature and density gradient driven modes in toroidal geometry. It is characterized by negative magnetic shear in the plasma interior and a peaked pressure profile. Stability to the ideal low-n external kink modes requires a conducting shell at 1.3 times the plasma minor radius. This novel plasma configuration is promising for improved plasma performance in advanced tokamak experiments.

Improvements in plasma performance are necessary to ensure the economic viability of tokamak reactors. We report here on a novel plasma configuration which improves simultaneously on three key plasma characteristics: the $\beta^* \equiv 2\mu_0\langle p^2\rangle_v^{1/2}/B_T^2$, which is a measure of the ratio of plasma kinetic pressure to toroidal magnetic field pressure and the fusion reactivity, the bootstrap (self-generated current) contribution to the plasma current, and the kinetic stability to toroidal drift-type modes. Here $\langle\cdot\rangle_v$ represents a volume average, p the plasma pressure, and B_T the vacuum toroidal magnetic field at the geometric center of the plasma. The units for all quantities are MKS unless otherwise noted. The definition of β^* can be contrasted with the more conventional form $\beta \equiv 2\mu_0\langle p\rangle_v/B_T^2$ by the additional weighting given to peaked pressure profiles, which will always make $\beta^* \geq \beta$. Both experiments and theoretical analyses have supported the empirical representation [1] of $\beta = \beta_N[I_p(\mathrm{MA})/aB_T]$ (or $\beta^* = \beta_N^*[I_p(\mathrm{MA})/aB_T]$), where the maximum β_N is determined by magnetohydrodynamics (MHD) stability. Here, I_p is the plasma current and a is the plasma minor radius. The MHD stability results will be given in terms of β_N^* and β_N.

The principal feature of this configuration is a region with significant negative magnetic shear $\propto dq/d\psi$, where ψ is a poloidal magnetic flux label, and $q(\psi)$ is the safety factor or inverse rotational number for the magnetic field in the plasma. The shear is negative over the central region of the plasma and then returns to the conventional positive shear near the plasma edge. The associated plasma current density is hollow. Negative magnetic shear has several beneficial effects. Among these are complete stability to $n = \infty$ ideal MHD ballooning modes in the negative magnetic shear region [2,3]. This implies that ballooning mode stability does not impose any constraint on the pressure gradient there. It permits strong peaking of the pressure profile, which can allow a large ratio of bootstrap to total plasma current, I_{bs}/I_p, and also produce a bootstrap current profile with favorable shape for stability. The hollow current profile associated with the negative magnetic shear enables raising q_{axis} without simultaneously raising q_{edge}, thereby allowing the plasma current to remain high. Raising q_{axis} is known to be beneficial to both low and $n = \infty$ instabilities [4,5]. Negative magnetic shear can also contribute to improved plasma confinement by acting to help suppress the primary destabilizing mechanisms for trapped particle modes [6].

Experimental discharges in JET [7] and DIII-D [8] have been produced that exhibit negative magnetic shear regions in the plasma center. These profiles are transient in nature and are the result of rapid elongation ramping in DIII-D and pellet injection in JET. The strong peaking of the pressure profiles observed within the negative magnetic shear region suggests the existence of a "transport barrier" (i.e., a localized region within the plasma where the thermal and particle transport are much smaller than in the surrounding regions). A principal difference between these experimental and the present configurations is the safety factor profile. The experimental cases have minimum safety factors about 1.0, thereby allowing the ideal $m = 1$ internal mode to be the dominant MHD instability. This is avoided in the present case by keeping the safety factor well above unity.

The limit on β_N^* is determined by stability to ideal MHD modes, particularly, the low-n external kink modes and the $n = \infty$ internal ballooning modes. The specific instability with the lowest β_N^* threshold depends sensitively on the plasma pressure and current profiles. When optimizing the plasma profiles to maximize β_N^*, two approaches have been pursued. The first achieves high pressure while keeping the plasma current as high as possible and results in relatively broad pressure and current profiles. This produces a low value for $\epsilon\beta_p$, where $\beta_p \equiv 2\mu_0\langle p\rangle_v/B_p^2$ and B_p is the poloidal magnetic field at the plasma edge. The second approach achieves high pressure by increasing the safety factor [4,5] throughout the plasma and consequently lowers the plasma current. This leads to a high value for $\epsilon\beta_p$, peaked profiles, and can allow complete stability to $n = \infty$ ballooning modes. We use a third approach where we increase the safety factor over most of the plasma cross section by creating a region with negative magnetic shear. This has the advantage of simultaneously allowing both high plasma
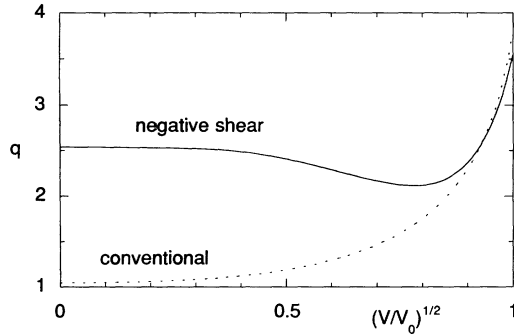
FIG. 1. The safety factor profiles for the negative magnetic shear (solid) and conventional shear (dotted) cases at β_N^* values of 6.3 and 5.1, respectively.
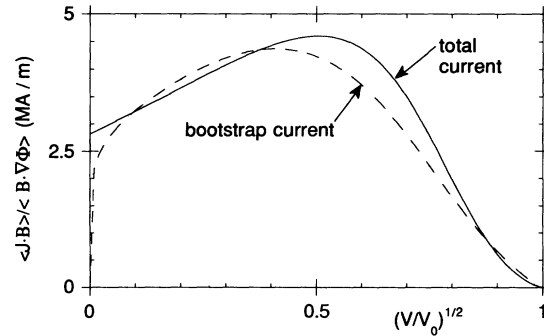
FIG. 2. Plasma parallel current density for negative magnetic shear case, showing the total (solid) and bootstrap (dashed) current profiles at $\beta_N^* = 6.3$.

current and peaked pressure profiles.

In this Letter we present the results of a study to optimize the plasma performance in the context of the Tokamak Physics Experiment (TPX) [9]. This experiment is intended to operate as a steady state tokamak at high β_N^*. The proposed device has a plasma aspect ratio of 4.5, vacuum toroidal magnetic field of 4.0 T, plasma current of 2.0 MA, and elongation and triangularity at the 95% flux surface of 1.8 and 0.5, respectively. In order to provide a comparison, results for both the negative magnetic shear configuration and a conventional shear configuration, which has positive magnetic shear throughout the plasma, will be given. The plasma equilibria for the two cases are shown in Figs. 1–3. Here the safety factor profiles and the parallel current density profiles ($\langle j \cdot B \rangle / \langle B \cdot \nabla \phi \rangle$) are plotted as a function of a minor radial coordinate, defined as the square root of the ratio of the volume enclosed by the flux surface to the total plasma volume. The brackets $\langle \cdot \rangle$ refer to the flux surface average. The pressure profiles are given by $p_0(1 - \hat{\psi})^{\alpha_p}$, where p_0 and α_p are 8.36×10^5 N/m^2 and 2.0 for the negative magnetic shear case, and 8.12×10^5 N/m^2 and 1.25 for the conventional shear case. The quantity $\hat{\psi}$ is the poloidal flux normalized to zero at the plasma axis and unity at the edge.

Ideal MHD stability analysis was carried out using BALMSC [3] for $n = \infty$ ideal MHD ballooning modes and PEST2 [10] for the low-n ideal MHD kink modes. The $n = \infty$ ballooning modes are found to be stable up to a β_N^* (β_N) value of 7.2 (5.5) for the negative magnetic shear case and 5.1 (4.0) for the conventional shear case. Above these values $n = \infty$ instability occurs in the region where the magnetic shear begins to rise rapidly near the plasma edge. We have examined the stability to $n = 1 - 6$ external kink modes with boundary conditions corresponding to a conducting shell at infinity and at $1.3a$, where a is the plasma minor radius. This shell position of $1.3a$ was chosen to represent the stabilizing effects of the conducting structures and vacuum vessel. For no conducting shell, the highest stable β_N^* (β_N) values for the negative

magnetic shear and conventional shear cases are 2.5 (1.9) and 4.2 (3.4), respectively. The limiting toroidal mode number is $n = 1$ for both cases. The negative magnetic shear case has a more peaked pressure profile and reduced magnetic shear near the plasma edge as compared to the conventional shear case. This leads to worse low-n stability in the absense of the conducting shell. However, for the more realistic conducting shell scenario, the values are 6.8 (5.2) and 5.2 (4.1), respectively. The limiting toroidal mode numbers in the presence of the conducting shell are $n = 3$ for the negative magnetic shear case and $n = 2$ for the conventional shear case. The enhanced stability of the negative magnetic shear configuration for $n \leq 6$ is due to a shifting of the mode structure from the plasma center to the region where the magnetic shear is zero, thereby bringing it closer to the conducting shell. Combining the results of the kink and ballooning stability, the β_N^* (β_N) limit is 6.8 (5.2) for the negative magnetic shear case and 5.1 (4.0) for the conventional shear case.

The plasma current is normally composed of a bootstrap and an external current drive component. Since methods for external current drive have low efficiencies, steady state tokamak operation will require that a large
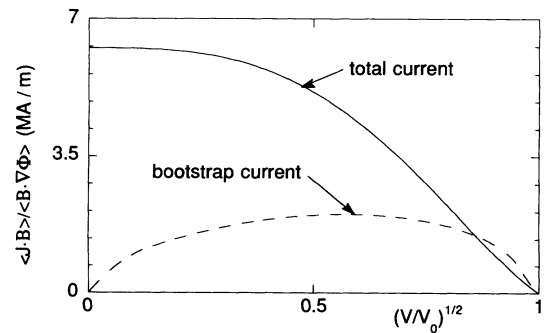
FIG. 3. Plasma parallel current density for the conventional shear case, showing the total (solid) and bootstrap (dashed) current profiles at $\beta_N^* = 5.1$.

fraction of the plasma current be generated by the bootstrap effect. The ratio of bootstrap current to total plasma current scales as $I_{bs}/I_p \approx C_{bs}\sqrt{\epsilon}\beta_p$, where C_{bs} depends primarily on the plasma density and temperature profiles [11], and $\epsilon = a/R$ is the plasma inverse aspect ratio. Hence, in order to achieve a large fraction, β_p and C_{bs} must be large. However, achieving a high ratio, $I_{bs}/I_p \approx 1$, alone is not sufficient because the resulting current and pressure profiles must be MHD stable. Since the shape of the bootstrap current profile is largely determined by the pressure gradient, it is naturally hollow. Profiles for the negative magnetic shear case and the conventional shear case are illustrated in Figs. 2 and 3, with the bootstrap current providing 93% and 50% of the total plasma current, respectively. Since the bootstrap ratio increases with β_N^*, although the negative magnetic shear case can access higher values, the β_N^* value is limited to 6.3 to maintain $I_{bs}/I_p \lesssim 1$. Values of total bootstrap current exceeding the desired plasma current are possible, and would require current drive opposite to the bootstrap current to remove the excess. The conventional shear case is at its stability limit of $\beta_N^* = 5.1$. For both cases the peak temperature is 20 keV, the effective ion charge is $Z_{eff} = 2.0$, and the Harris collisional model [12] is used to estimate the bootstrap current contribution. The temperature and density profiles are shown in Fig. 4. For the negative magnetic shear case, the bootstrap and total current profiles are very closely aligned and demonstrate that the bootstrap effect can provide nearly 100% of the plasma current with a profile that has favorable MHD stability properties.

In order to address the effect of negative magnetic shear on confinement, a comprehensive kinetic toroidal eigenvalue calculation [13,14] is employed to investigate the linear stability of toroidal drift-type modes. The analysis includes dynamics associated with the most prominent microinstabilities: the ion temperature gradient [$\eta_i \equiv (d\ln T_i/dr)/(d\ln n_i/dr)$] modes and the trapped particle modes. For sufficiently large negative magnetic shear, the orbit-averaged magnetic curvature and gradient drifts change from destabilizing to stabilizing for the majority of the trapped particles, so that enhanced confinement may be expected. Although this effect of negative magnetic shear on trapped particle instabilities is well known [6], until recently the means for creating such large negative magnetic shear in tokamaks was not established. The other dominant destabilizing mechanism for toroidal drift modes is the ion temperature gradient, parametrized by η_i. For typical tokamak parameters, suppression of this mechanism requires $\eta_i < \eta_i^{crit}$, with η_i^{crit} in the range from 1 to 2 [15]. It is important to note that the density and temperature profiles, which optimize the bootstrap current for the negative magnetic shear equilibrium reported here, correspond to $\eta_i < \eta_i^{crit}$ in the same region of the plasma interior where $s \lesssim 0$. Figure 5 illustrates the radii where s has a minimum and η_i has a minimum. For the present discussion of plasma transport the definition of magnetic shear will be $s \equiv (r/q)dq/dr$, where r is the (horizontal) flux surface minor radius. Between these two locations there is a completely stable region for the toroidal drift-type instabilities. The linear growth rates for the negative magnetic shear and conventional shear cases are shown in Fig. 6. Here it is seen that kinetic stability for the negative magnetic shear case occurs in the region where the conditions that $s \lesssim 0$ and $\eta_i < \eta_i^{crit}$ are simultaneously satisfied, while the conventional shear case exhibits a finite growth rate throughout the plasma.

The toroidal drift-type instabilities analyzed here are acknowledged to be leading candidates to account for the anomalous radial transport of particles and energy observed in the interior region of tokamak experiments [16]. If these modes can be linearly stabilized by the profiles that generate negative magnetic shear, then the transport in the stabilized region should be reduced to the neoclassical (collisional) level. This effectively forms a "transport barrier" in the plasma interior which can sustain the peaked pressure profiles, shown here to be
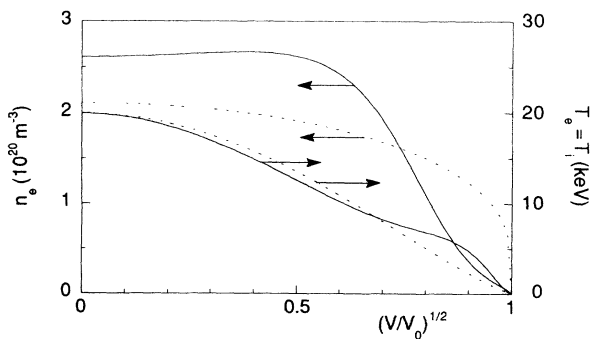
FIG. 4. The plasma temperature and density profiles for the negative magnetic shear case (solid) and the conventional shear case (dotted).
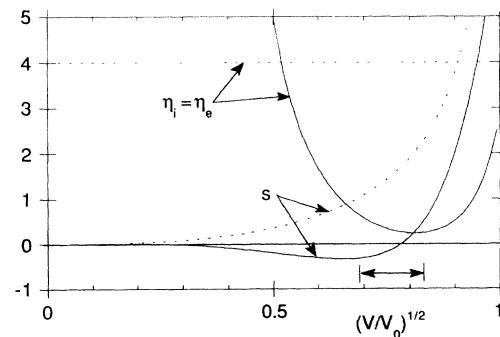
FIG. 5. The magnetic shear $s \equiv (r/q)dq/dr$ and $\eta_i \equiv (d\ln T_i/dr)/(d\ln n_i/dr)$ profiles for the negative magnetic shear case at $\beta_N^* = 6.3$ (solid), and the conventional shear case at $\beta_N^* = 5.1$ (dotted). The stable region for the negative magnetic shear case is also indicated.
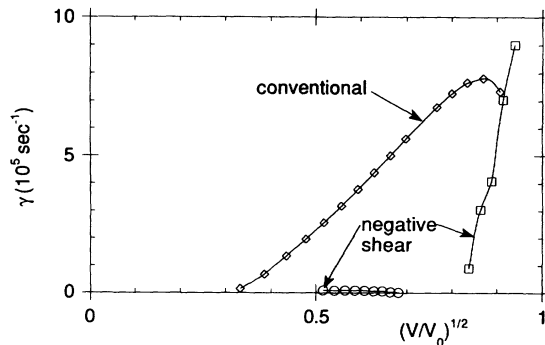
FIG. 6. The linear growth rates of the toroidal drift mode, for the negative magnetic shear and conventional shear cases, calculated in the electrostatic limit. Here, $k_\theta \rho_i$ is chosen to approximately maximize the growth rate, and collisions and a carbon impurity are included in the calculation.

advantageous to both ideal MHD stability and bootstrap current generation.

The present analysis has identified a target configuration for improved tokamak performance, which is the critical first step for guiding experimental and theoretical analysis. Work on simulating the dynamic evolution of the negative magnetic shear configuration is planned, since this is essential for establishing its accessibility in experiments.

In summary, we have reported on the favorable properties of tokamak plasmas with negative magnetic shear in the plasma center. These include a near 100% self-generated current profile, excellent stability to ballooning modes, and a possibility of enhanced confinement through suppression of toroidal drift-type instabilities. The external kink modes are the limiting instability and require additional stabilization through the presence of a conducting shell at approximately 1.3 times the minor radius. Work on the resistive MHD modes is underway and will be reported elsewhere.

[1] F. Troyon and R. Gruber, Phys. Lett. 110A, 29 (1985).
[2] A. Sykes and M. F. Turner, in Proceedings of the 9th European Conference on Controlled Fusion and Plasma Physics, Oxford, 1979 (Culham Laboratory, Abingdon, England, 1979), p. I-161.
[3] M. S. Chance and J. M. Greene, Nucl. Fusion 21, 453 (1981).
[4] M. J. Gerver, J. Kesner, and J. J. Ramos, Phys. Fluids 31, 2674 (1988).
[5] A. Sykes, J. A. Wesson, and S. J. Cox, Phys. Rev. Lett. 39, 757 (1977).
[6] B. B. Kadomtsev and O. P. Pogutse, Zh. Eksp. Teor. Fiz. 51, 1734 (1966) [Sov. Phys. JETP 24, 1172 (1967)].
[7] M. Hugon et al., Nucl. Fusion 32, 33 (1992).
[8] E. A. Lazarus et al., Phys. Fluids B 3, 2220 (1991).
[9] R. J. Goldston et al., in Proceedings of the 20th European Conference on Controlled Fusion and Plasma Physics, Lisbon, 1993 (European Physical Society, Lisbon, Portugal, 1993), p. I-319.
[10] R. C. Grimm, R. L. Dewar, and J. Manickam, J. Comput. Phys. 49, 94 (1983).
[11] N. Pomphrey, Report No. PPPL-2854, August, 1992 (unpublished).
[12] G. R. Harris, Report No. EUR-CEA-FC-1436, November, 1991 (unpublished).
[13] G. Rewoldt, W. M. Tang, and M. S. Chance, Phys. Fluids 25, 480 (1982).
[14] G. Rewoldt, W. M. Tang, and R. J. Hastie, Phys. Fluids 30, 807 (1987).
[15] G. Rewoldt and W. M. Tang, Phys. Fluids B 2, 318 (1990).
[16] P. C. Liewer, Nucl. Fusion 25, 543 (1985).